Colloid Polym Sci (2006) 284: 795–801
DOI 10.1007/s00396-005-1456-5

ORIGINAL CONTRIBUTION

Irina Nikolaevna Topchieva
Vasily Vladimirovich Spiridonov
Nadezhda Anatol'evna Kataeva
Sergey Pavlovich Gubin
Sergey Konstantinovich Filippov
Andrey Vladimirovich Lezov

Magnetic nanocomposites based on cyclodextrin-containing molecular tubes and iron nanoparticles

Received: 4 May 2005
Accepted: 11 November 2005
Published online: 22 March 2006

I. N. Topchieva ·
V. V. Spiridonov (✉)
Chemical Department,
Moscow State University,
Leninsky gory, GSP-3,
Moscow 119899, Russia
e-mail: kurganov@gagarinclub.ru
Tel.: +7-095-9393127
Fax: +7-095-9390174

N. A. Kataeva · S. P. Gubin
Kurnakov Institute of General and
Inorganic Chemistry,
Leninsky pr., 31,
Moscow 119991, Russia

S. K. Filippov · A. V. Lezov
Department of Polymer Physics,
Saint-Petersburg State University,
Ulyanovskaya str., 1,
St. Petersburg 198904, Russia

Abstract Stabilization of metallic nanoparticles may be achieved by the formation of their adducts with polymers and/or nanotubes of various chemical composition. Here, water-soluble nanotubes based on β-cyclodextrin (β-tubes) were used for entrapping of Fe nanoparticles obtained by the reduction of iron-containing precursors ($[Fe_3(CO)_{11}H][Et_4N]$ cluster and $FeSO_4$). Using methods of light-scattering, viscometry, and isothermal diffusion measurements, it was shown that the adducts are associated in aqueous solutions. The presence of iron nanoparticles and the shape and size of adducts were verified by transmission electron microscopy. The adducts are long (up to 600 nm and longer), translucent associates consisting of denser walls and transparent cores. The width of nanotubes is ~150 nm and the thickness of the wall 3–25 nm. Their magnetic properties were demonstrated by electron paramagnetic resonance method. The mechanism of self-assembly of the adducts is discussed.

Keywords Cyclodextrin nanotubes · Iron-containing nanocomposites · Magnetic nanoparticles · Dynamic light scattering · Transition electron microscopy · Electron paramagnetic resonance

Introduction

There has been considerable interest in the exploitation of new materials for magnetic record of information. For this purpose, the films based on iron nanoparticles: α-Fe, γ-Fe_2O_3, and Fe_2O_3–Fe_3O_4 with the thickness of 5–10 nm are usually used [1].

Plenty of methods are known for the synthesis of iron nanoparticles: thermolysis of iron-containing organic compounds [2], ultrasonic decomposition of iron carbonyl in the presence and absence of surface active compounds [3, 4], and the method of electrochemical generation [5]. These methods result in the formation of nanoparticles composed of the oxides of iron. Using the method of laser evaporation of the metal, the nanoparticles of α-Fe and γ-Fe were received [6]. The electroarc method of decomposition $Fe(CO)_5$ results in the formation of threadlike nanoparticles of α-Fe [7]. Another way to achieve zero-valent iron formation is the chemical reduction of salts based on bivalent iron in soles of SiO_2 [8].

For the stabilization of nanoparticles, the monolayers of surface active compounds [9], synthetic carbo- and heterochained polymers [10–13], and ion exchange pitches are used [14].

A new approach for the stabilization of nanoparticles is their inclusion in tubular structures. Over the past decade, major advances have been made in the synthesis of new

tubular nanostructures. One can now synthesize the carbon-based nanotubes [15] as well as a big family of inorganic tubes based on nitride boron [16], sulfides of molybdenum, tungsten [17], etc.

Last time, a novel type of nanotubes that presented structures composed of cyclic compounds, called cyclodextrins (CD), as starting materials are described [18–23]. In this case, one may receive water-soluble nanotubes with expected dimensions of inner cavity that are capable of binding guests of appropriate size, shape, and polarity.

The synthesis of nanotubes based on α-CD (α-tubes) was first fulfilled by Harada et al. [18], using the combination of methods of supramolecular chemistry (synthesis of polyrotaxanes) and chemical modification of polymers. The authors described inclusion complexes between α-tubes and I^{3-} [18]. In the subsequent works in this field, molecular mass characteristics [19, 20] and complexation properties of α-tubes using alkyl suphonates [19, 21], polyanilyne [20] poly(ethylene glycol) [22] as ligands were studied.

In this work, we used nanotubes based on β-CD (β-tubes) synthesized by the modified method eliminating the stage of polyrotaxane synthesis [23].

One of the most important properties of nanotubes, which was demonstrated using carbon nanotubes as an example, is their ability to perform matrix synthesis of nano-threaded materials from other substances including metals such as Fe, Co, Mn, etc. [24]. It allows the receipt of hybrid nanocomposites containing both organic and inorganic components. The inclusion of metal nanoparticles favors the stability of metals in oxidation processes due to their full or partial coverage by organic molecules. These materials have several unusual and potentially useful properties combining electric, magnetic, and catalytic ones inherent to inorganic compounds, as well as dielectric properties inherent to substances of organic origin. It makes them promising objects for many applications in optics [25], electronics [26], and biodiagnostics [27].

It is known [28] that carbohydrates are able to form complexes with metal ions due to the formation of ionic coordination bonds with deprotonated hydroxyl groups. For instance, Fe^{3+} forms complexes of such high stability that precipitation of even some least soluble hydroxides, namely, $Fe(OH)_3$/FeO(OH) is prevented in the presence of some carbohydrates. Fe^{2+}, being a less acidic species, does not form complexes with sugars [28].

In this respect, it is important to investigate the mode of interaction between β-tubes and metals forming during the reduction of Fe precursors to clarify the principal regularities in their structure formation: if the metals form nanowires included in the cavity of tubes or these structures can be self-organized into other type of architectures.

For this purpose, we carried out the synthesis of the adducts between β-CD-based nanotubes (Fig. 1) and iron, bearing in mind to study the structure in the solution and condensed phase.

Experimental

The preparation of the adducts described in [29] was performed in three stages. The first stage is the formation of the inclusion complex based on di*block* polyethylene and polypropylene oxide copolymer and β-CD [30]. (The percentage of polypropylene oxide in *block*-copolymer is 40%. The molecular weight of the copolymer is 3,600.) The second stage is the cross-linking of β-CD units by epichlorohydrin and dethreading of the polymer [23]. The molecular mass of β-tubes corresponds to 4,500 (tetramer) and M_W/M_N is 1.02 [23].

The last stage of the synthesis of Fe containing adducts based on β-tubes was performed in two methods.

1. In 500 ml of C_2H_5OH H_2O (4:1) solution, 0.7 g of $[Fe_3(CO_{11})H][Et_4N]$ was dissolved and the solution of β-tubes was added (the molar ratio of β-tubes $[Fe_3(CO_{11})H][Et_4N]$ is 1:10). The solution was allowed to stand in air until complete discoloration and precipitation of iron hydroxide was achieved (usually ~7 days). The Fe content in the adduct was 0.1%.
2. To the solution containing β-tubes (75 mg, 0.066 mM) and $FeSO_4{\cdot}5\ H_2O$ (0.66 M) in 50 ml of 0.1 M NaOH sodium hypophosphite was added. Molar ratio of $FeSO_4$ to NaH_2PO_2 is 1:1, while molar ratio of $FeSO_4$ to β-tubes (per CD unit) is 10:1. The reaction was carried out in an inert atmosphere: The solution of

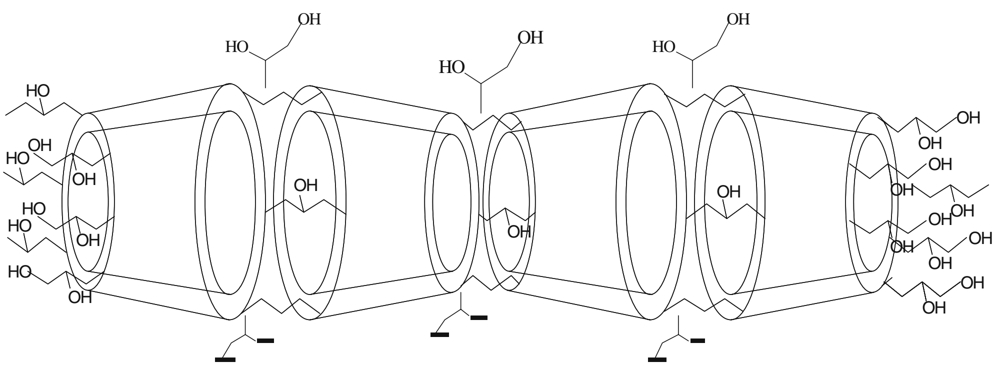

Fig. 1 Chemical structure of hollow β-tubes

sodium hypophosphite was added drop by drop to a vigorously stirred solution of $FeSO_4$. The end of the reaction was taken to be the completion of Fe hydroxide deposition. The Fe content in the adduct was 1.1%.

The separation of desired products was carried out using the dialysis through cellulose tubing following by gel permeation chromatography using Sephadex G50 (coarse) as a support and water as an eluent. The yield of product is 20–25%.

IR spectra were recorded in the range 4,000–400 cm^{-1} using a Specord-75 photometer. Spectra of electron paramagnetic resonance (EPR) were recorded using a Varian E 4 radiospectrometer in X-range (operating frequency=9.2 GHz) at 300 K.

The experiments on the titration of β-tubes and the adducts with phenolphtalein (PP) were made as described in [23, 29].

The content of iron was defined spectrophotometrically. Seven milligrams of the adduct were dissolved in 0.01 M H_2SO_4 while heated for 3–5 min, and 10 ml of 2-hydroxy-5-sulphobenzoic acid (10% solution) was added. The absorbance of the complex was registered at λ=510 nm (the extinction coefficient, ε, equals to 1,900 l/mol cm) [30]. The quantity of iron was determined from the calibration plot (D vs C plot, where D is the absorption of the complex solution and C is the concentration of $FeCl_3$) [29, 31].

The weight percent of iron was calculated from the equation:

$$\eta = (m/p) * 100\%$$

where m is the mass of iron at specimen and p is the mass of adduct.

Dynamic light scattering studies

The measurements of dynamic light-scattering were performed using photon correlation spectroscopy method of the "Photocor Instruments" apparatus. The sample was illuminated by linear polarized light of He–Ne laser with the wavelength λ=632.8 nm. Autocorrelation function of intensity of scattering light g_2 was measured in the regime of photon count in the range of scattering angles, θ, from 25 to 90°. The analysis of autocorrelation function was performed using the DynaLS program, giving the distribution functions

Table 1 The values of diffusion coefficients, hydrodynamic radii, and specific viscosity for adducts and β-tubes

Sample	Composition	[η], dl/g	K'	$D\times10^7$, sm^2/s	R_h, nm
1	Fe adduct	0.040	7.3	0.11	209.0
2	β-tubes	0.076	1.8	5.70	4.3

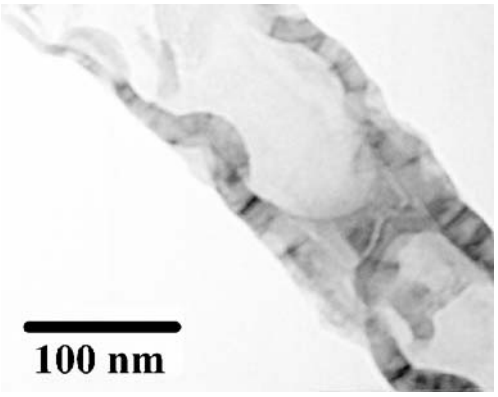

Fig. 2 TEM image of adduct β-tubes with iron

with respect to their hydrodynamical radii (R_h) or times of relaxation $1/\tau=Dq^2$, where D is the coefficient of translational diffusion of particles. As all the observed modes display diffusion character ($1/\tau \sim Dq^2$), the values of coefficients D were calculated from the slope of linear dependence of relaxation rate $1/\tau$ vs scattering vector squared, q^2. Hydrodynamic radius of particles, R_h, was calculated using Stock's equation for solid particles of spherical shape [32]:

$$D = \frac{kT}{6\pi\eta_o R_h}$$

where η_0 is the solvent viscosity, k is the Bolzman's constant, and T is the temperature.

Viscosity measurements

Viscosity of aqueous solutions for the adduct and β-tubes were measured using Ostwald's capillarity viscosimeter at T=294 K. Intrinsic viscosity [η] was calculated by the extrapolation of specific viscosities for a series of 4–5 concentrations (1–3%) to the zero concentration.

Results and discussion

Iron-containing adducts were synthesized by two methods: photochemical decomposition of $[Fe_3(CO_{11})H][Et_4N]$ and

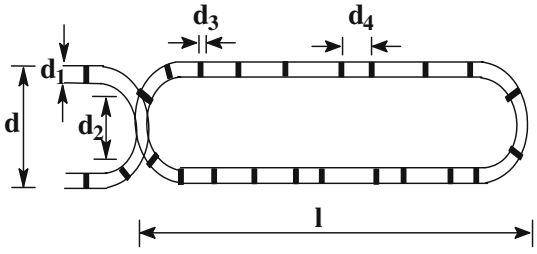

Fig. 3 The model of the adduct structure

Table 2 Sizes of adducts obtained by different methods

	Hollow nanotubes, nm	Filled nanotubes (Fe from $[Fe_3(CO)_{11}H][Et_4N]$), nm
The length of tube fragment	300–600	200–450
Tube thickness (d)	60–150	30–140
Wall thickness (d_1)	5–25	3–25
Bridge thickness (d_2)	50–100	20–70
Width of the zone filled with iron (d_3)		3–10
Distance between filled zones (d_4)		4–15

the reduction of $FeSO_4$ by NaH_2PO_2 in the presence of β-tubes. The data of IR spectroscopy show that samples of adducts obtained by the first method do not contain bands of carbonyl groups in the field 2,100–1,700 cm^{-1}. It indicates that the adduct does not contain the CO ligands.

The comparison of the solubility of adducts and β-tubes in water shows that the adducts have much lesser solubility. It means that the formation of the adduct is accompanied by the aggregation of the particles.

For the determination of the size and shape of the adduct particles, the methods of photon correlation spectroscopy and viscosity were used. Thus, the distribution functions of translational diffusion coefficients D_t for solutions of adducts and original β-tubes at different concentrations and different angles were obtained. The distribution function $W(D_t)$ for the adduct is characterized with one broad peak. Its position shifts to bigger values of D_t with a decrease of the solution concentration.

The values of diffusion coefficients, D_0, were determined for adducts and β-tubes by the extrapolation of concentration dependencies of the diffusion coefficient to infinite dilution. The calculation of the values of hydrodynamic radii, R_h, for adducts and β-tubes gives the values 214 nm (for the adduct) and 4.3 nm (for β-tubes) using the Stock's equation. These significant radii discrepancy indicates that the iron-containing adduct exists in solution in the form of associates. This is in accordance with extraordinary high value of Huggins constant K' value and small value of intrinsic viscosity $[\eta]$ for adducts (Table 1). Indeed, K' values depend on the conformation of the molecules and the thermodynamic quality of the solvent and describe the interaction between macromolecules in the solvent. The association of the molecules results in the increase of Huggins constant up to the value higher than 1. Probably, the driving force of association is the formation of the hydrogen bonds between hydroxyl groups of CD residues. The values of diffusion coefficients, hydrodynamic radii, Huggins constant K', and intrinsic viscosity $[\eta]$ for the adduct and β-tubes are presented in Table 1.

It is seen that a substantial difference in hydrodynamic properties of the adduct and β-tubes is already revealed in the range of low concentrations. One may suppose that the inclusion of iron results in the "cross-linking" of molecular tubes or their associates accompanied by the formation of large aggregates. This hypothesis could be verified by the estimation of molecular mass for the adduct $\left(MD_{\eta\,\mathrm{add}}\right)$ and β-tubes in the form of associate $\left(M_{D\eta\,\mathrm{tube}}\right)$, respectively, on the basis of the following relationship [33, 34]:

$$\frac{M_{\mathrm{add}}}{M_{\mathrm{tube}}} = \frac{[\eta]_{\mathrm{tube}}}{[\eta]_{\mathrm{add}}}\left(\frac{D_{\mathrm{tube}}A_{0,\mathrm{tube}}}{D_{\mathrm{add}}A_{0,\mathrm{add}}}\right)^3$$

Here, A_0 is so-called hydrodynamic invariant for the adduct and β-tubes, respectively. For polymers, the specific value of A_0 is varying from 3.2×10^{-10} to 3.8×10^{-10} erg/K $mol^{1/3}$ [35]. The estimated ratio was $MD_{\eta\,\mathrm{add}}/M_{D\eta\,\mathrm{tube}}$ about 350,000 if we assume that A_0 is identical for the adduct and β-tubes. However, even if this assumption is not true, the estimated ratio will be of the same order of magnitude due to a minor variation of A_0.

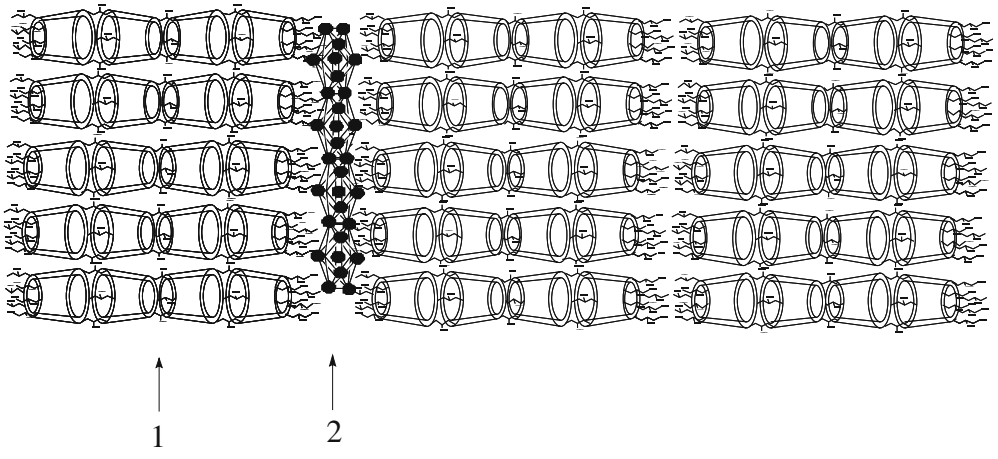

Fig. 4 Schematic representative of a fragment of the adduct wall. *1* β-tubes, *2* Fe nanoparticles

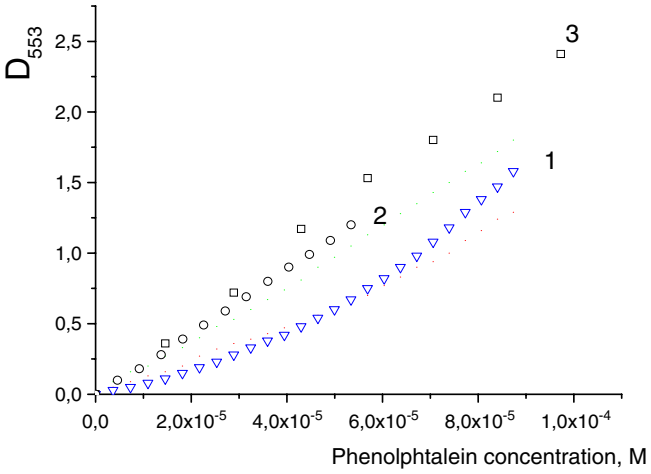

Fig. 5 Titration curves of: *1* hollow β-tubes, C=1.5×10^{-3} M (per β-CD unit); *2* β-tubes*Fe, C=1.5×10^{-3} M (per β-CD unit), and *3* pure phenolphthalein

To verify the presence of Fe-containing nanoparticles inside β-tubes and the dimensions of hollow and filled tubes in condensed state, we used transmission electron microscope (TEM) (Fig. 2).

In both cases, one may observe long (up to 250 nm and longer) translucent objects consisting of denser walls and transparent cores and having bridges at intervals. The width of nanotubes is about 100 nm and the thickness of the wall is about 3–5 nm.

The TEM images of the adduct show that the walls of nanotubes contain darker zones corresponding to the adsorption of electrons by heavy nuclei (Fe). They look like the dark crossbars located across the walls of nanotubes. It is seen that TEM patterns observed are independent of the type of precursor and the method of Fe reduction. With our findings as basis, we suggested the model of the adduct structure that is depicted in Fig. 3. (The data of the dimensions of both types of nanotubes are presented in Table 2).

Fe-containing nanoparticles have a nonspherical form. Their length varies from 3 to 25 nm, while their thickness from 3 to 10 nm. We may assume that the β-tube unimers form stacks that are parallel to the nanotube length. In the course of the reduction of iron precursors, iron atoms should at least partially fit into the β-tube cavity due to hydrophobic interactions; therefore, the iron clusters should be perpendicular to the tube length (Fig. 4).

The additional evidence in favor of this type of iron nanoparticles arrangement was received from the data of spectrophotometric titration by dyes. It is known that β-CD is able to form inclusion complexes with PP [36]. The same property is inherent to the end groups of β-tubes [23]. One may assume that due to the blocking of the end groups of β-tubes by nanoparticles, the end groups would be inaccessible for the interaction with PP. Indeed, it was shown that the adduct has practically lost its ability to bind the dye (Fig. 5).

The existence of Fe nanoparticles in the adducts is also supported by the magnetic characteristics of the samples synthesized from both types of Fe precursors. The residual magnetization of the sample was measured using EPR method. Figure 6a shows the spectrum of ferromagnetic resonance in the sample of the adduct synthesized from [$Fe_3(CO_{11})H$][Et_4N]. The spectrum consists of two broad lines characterized with the effective g-factors ~6–8 and ~2–3, that demonstrates the presence of ferromagnetic nanoparticles in the sample.

Figure 6b shows the dependence of the signal of microwave absorption of the first derivative from the outer magnetic field (H) at the increase of H (up to 3$k\Theta$) and subsequent decrease (up to 0). The hysteresis observed in this plot indicates nonzero residual magnetization of the sample. We suggested, based on these data, that observed ferromagnetism may be intrinsic of Fe nanoparticles in the adducts. EPR spectra of the adduct system obtained from $FeSO_4$ (not shown) demonstrate that the samples are

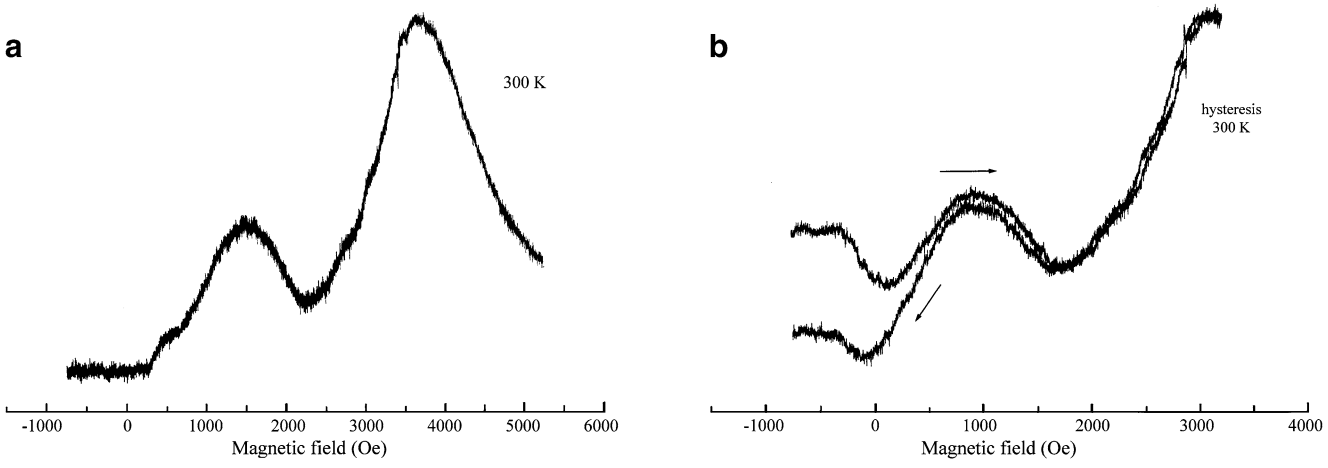

Fig. 6 **a** EPR spectrum of the adduct prepared from the cluster [$Fe_3(CO_{11})H$][Et_4N] at room temperature. **b** The dependence of the signal of microwave adsorption of the first derivative from the outer magnetic field

present in the superparamagnetic state at room temperature. Basing on the existence of two intensive lines in spectra and the form of lines testifying high electroconductivity of the sample (Fig. 6a), one may suppose that Fe nanoparticles consist from two species, i.e., Fe^0 surrounded by iron oxides.

It is important to note that the formation of adducts with iron is observed only in the case when CDs are organized in columnar structures. Indeed, special experiments on the reduction of Fe precursors show that CD and some of its commercial derivatives do not reveal the ability to form adducts with Fe. It may be regarded as the indirect indication that the formation of nanocomposites is not accompanied with the inclusion of metal nanoparticles in the cavity of CD. The same conclusion was drawn in Huang et al. [37], where it was shown that nanoparticles of gold are not included in β-CD cavities. Besides, the analysis of the structure of the adduct based on γ-Fe_2O_3 and γ-CD manifested that these adducts present nanoparticles of γ-Fe_2O_3 entrapped in tiny pseudosingle crystals of γ-CD [38].

The conclusion about the structure of adducts based on TEM data favor to draw an analogy between the formation of the structure of two-component nanocomposites consisting of greatly differing components, and *block* copolymers. It is known that in the last case, self-organization occurs via the phase segregation in a way that would align the structures to maximize interactions between blocks of similar composition [39].

The key property of adducts is the stability of Fe nanoparticles in the oxidation process, shown in the fact that aqueous solutions do not change their color and remain transparent even under the long storage in air. One may suggest that one of the reasons of chemical stabilization of Fe nanoparticles in adducts is the protective effect of the dense "coat" from 2,3-dihydroxypropyl substituents attached to terminal CD molecules of β-tubes.

Thus, the studied system of the adduct based on CD-containing nanotubes and Fe nanoparticles presents the example of nanocomposites characterized by a specific two-phase structure. It is possible that this structural motif is inherent to some other types of nanocomposites based on tubular compounds and metals.

Conclusion

It is established for the first time that nanocomposites based on cyclodextrin form long nanotubes, have semitransparent formations consisting of denser walls and transparent cores. Iron nanoparticles build in the walls of nanotubes perpendicular to the tube length. Based on structural characteristics of the adducts, an analogy between the principles of the formation and self-organization of *block* copolymers was drawn. In both cases, these compounds are formed via the phase segregation in a way that would greatly align the structures to maximize interactions between differing blocks.

Acknowledgements We are grateful to V. A. Kabanov for fruitful discussions, E. I. Ryumtsev for his interest in our study, G. Yu. Yurkov for the assistance with the TEM experiments, Yu. A. Koksharov for supplying the results of EPR study of materials and fruitful discussions, G. A. Tsirlina and V. M. Ivanov for their interest and helpful discussions, and F. A. Kalashnikov for the assistance in preparing the manuscript.

This work was supported by the Russian Foundation for Basic Research (project nos. 05-03-32083, 04-03-32090, and 04-03-32750), the International Science and Technology Center (project no. 1991), and the programs of the Presidium of the RAS "Fundamental Problems of Physics and Chemistry of Nanosized Systems and Nanomaterials" and "Directed Synthesis of Inorganic Substances with Specified Properties and Design of Functional Materials on Their Basis."

References

1. Gubin SP, Koksharov Yu A, Khomutov Yu A, Yurkov G Yu (2005) Uspekhi khimii 74:539
2. Matur S, Veith M, Sivakov V, Shen H, Huch V, Hartman U, Gao HB (2002) Chem Vap Depos 8:277
3. Suslick KS, Fang M, Hyeon T (1996) J Am Chem Soc 118:11960
4. Prozorov T, Kataby G, Prozorov R, Gedaken A (1999) Thin Solid Films 340:189
5. Pascal C, Pascal JL, Favier F, Moubtassim MLE, Payen C (1999) Chem Mater 11:141
6. Haneda K, Zhou ZX, Morrish AH, Majima T, Miyahara T (1992) Phys Rev B 46:13832
7. Okotrub AV, Kuznetsov VL, Sharaya A, Butenko Yu V, Chuvilin AL, Shubin Yu V, Varnek VA, Klein O, Pascard H (2002) Chemistry for Sustainable Development: 10:781
8. Bose P, Bid S, Pradhan SK, Pal M, Chakravorty D (2002) J Alloys Compd 343:192
9. Fu L, Dravid VP, Johnson DL (2001) J Appl Surf Sci 181:173
10. Smith TW, Wychick D (1980) J Phys Chem 84:1621
11. Gubin SP, Korobov MS, Yurkov G Yu, Tsvetnikov AK, Buznick VM (2003) Dokl Akad Nauk 388:493
12. Gubin SP, Yurkov G Yu, Korobov MS, Koksharov Yu A, Kozinkin AV, Pirog IV, Zubkov SV, Kitaev VV, Sarichev VM, Buznick VM, Tsvetnikov AK (2005) Acta Mater 53:1407
13. Habibullina NR, Jeglov EP, Shulyndin SV (2000) Theses of International Conference "Mossbauer effect: magnetism. Materials science: gamma-optics", Kazan, Russia, 26 June–1 July 2000, p 155
14. Tesla AM, Foglia S, Suber L, Fiorani D, Casas L, Roig A, Molins E, Greneche JM, Tejada J (2001) J Appl Phys 90:1534

15. Iijima S (1991) Nature 354:56
16. Yu DP, Sun XC, Lee CS et al (1966) Appl Phys Lett 72:1966
17. Tenne R, Margulis L, Genut M, Hodes G (1992) Nature 360:444
18. Harada A, Li J, Camachi M (1993) Nature 364:516
19. Ikeda T, Ooya T, Yui N (2000) Polym Adv Technol 11:830
20. Maarten van den Boogaard (2003) Cyclodextrin-containing supramolecular structures: from pseudopolyrotaxanes toward molecular tubes, insulated molecular wires and topological networks. University Library Groningen, Netherlands
21. Ikeda T, Hirota E, Ooya T, Yui N (2001) Langmuir 17:234
22. Ikeda T, Okumura Y, Shimomura T, Ito K, Hayakawa R (2000) J Chem Phys 112(9):4321
23. Topchieva IN, Kalashnikov Ph A, Spiridonov VV, Melnikov AB, Polushina GA, Lezov AV (2003) Dokl Akad Nauk 399(1–3):115
24. Zhang GL et al (1996) Appl Phys 80:579
25. Ahmad K, Henikoff S (2002) Proc Natl Acad Sci U S A 99[Suppl 4]:16447
26. Clarkson MJ, Wells JRE, Gibson F, Saint R, Tremethick DJ (1999) Nature 399:694
27. Hatch CL, Bonner WM, Moudrianakis EN (1983) Science 221:468
28. Geibelmann A, Clufers P, Kropfgans C, Mayer P, Piotrowski H (2005) Angew Chem Int Ed Engl 44:924
29. Topchieva IN, Spiridonov VV, Kataeva NA, Gubin SP, Filippov SK, Lezov AV (2004) Dokl Akad Nauk 399(1–3):219
30. Panova IG, Gerasimov VI, Grokhovskaya TE, Topchieva IN (1996) Dokl Akad Nauk 347:61
31. Zolotov Yu A (2001) The foundations of analitycal chemistry. Vysshaya Shkola, Moscow
32. Tsvetkov VN, Eskin VE, Frenkel S Ya (1964) Structure of macromolecules at the solutions. Nauka, Moscow
33. Tsvetkov VN (ed) (1989) Rigid-chain polymers: hydrodynamic and optical properties in solution (Macromolecular compounds). Consultants Bureau, New York
34. Bakeev KN, Shu YM, Zezin AB, Kabanov VA, Lezov AV, Mel'nikov AB, Kolomiets IP, Rjumtsev EI, MacKnight WJ (1996) Macromolecules 29(4):1320
35. Zimm B, Crothers D (1962) Proc Natl Acad Sci U S A 48(6):905
36. Sasaki KJ, Christian CSD, Tucker EE (1989) Fluid Phase Equilib 49:281
37. Huang Y, Li D, Li J (2004) Chem Phys Lett 389:14
38. Bonacchi D, Caneschi A, Dorignac D et al (2004) Chem Mater 16:2016
39. Hadjichristidis N, Pispas S, Floudas G (2003) Block copolymers: synthetic strategies, physical properties, and applications. Wiley, New York